

## Stretching of Single Collapsed DNA Molecules

Christoph G. Baumann,\* Victor A. Bloomfield,\* Steven B. Smith,<sup>†</sup> Carlos Bustamante,<sup>†‡</sup> Michelle D. Wang,<sup>§</sup> and Steven M. Block<sup>§</sup>

\*Department of Biochemistry, University of Minnesota, St. Paul, MN 55108; <sup>†</sup>Department of Molecular and Cell Biology, University of California, Berkeley, CA 94720; <sup>‡</sup>Department of Physics, University of California, Berkeley, and Physical Biosciences Division, Lawrence Berkeley Laboratory, Berkeley, CA 94720; and <sup>§</sup>Department of Molecular Biology, Princeton University, Princeton, NJ 08544

**ABSTRACT** The elastic response of single plasmid and lambda phage DNA molecules was probed using optical tweezers at concentrations of trivalent cations that provoked DNA condensation in bulk. For uncondensed plasmids, the persistence length,  $P$ , decreased with increasing spermidine concentration before reaching a limiting value 40 nm. When condensed plasmids were stretched, two types of behavior were observed: a stick-release pattern and a plateau at  $\sim 20$  pN. These behaviors are attributed to unpacking from a condensed structure, such as coiled DNA. Similarly, condensing concentrations of hexaammine cobalt(III) (CoHex) and spermidine induced extensive changes in the low and high force elasticity of lambda DNA. The high force (5–15 pN) entropic elasticity showed worm-like chain (WLC) behavior, with  $P$  two- to fivefold lower than in low monovalent salt. At lower forces, a 14-pN plateau abruptly appeared. This corresponds to an intramolecular attraction of 0.083–0.33 kT/bp, consistent with osmotic stress measurements in bulk condensed DNA. The intramolecular attractive force with CoHex is larger than with spermidine, consistent with the greater efficiency with which CoHex condenses DNA in bulk. The transition from WLC behavior to condensation occurs at an extension about 85% of the contour length, permitting looping and nucleation of condensation. Approximately half as many base pairs are required to nucleate collapse in a stretched chain when CoHex is the condensing agent.

### INTRODUCTION

DNA undergoes ordered collapse, or condensation, in dilute solution in the presence of multivalent cations such as spermidine<sup>3+</sup>, hexaammine cobalt(III), and spermine<sup>4+</sup> (Gosule and Schellman, 1976; Widom and Baldwin, 1980; Wilson and Bloomfield, 1979). The toroidal condensed state is similar to the structure of packaged bacteriophage DNA, and some of the physical interactions involved in DNA condensation, such as bending, entropy loss, and modification of coulombic interactions must also be involved in DNA packaging in eukaryotic nuclei and prokaryotic nucleoids (see reviews by Bloomfield, 1991, 1996, 1997; Marquet and Houssier, 1991). Theory predicts that DNA collapse will involve an abrupt phase transition (Grosberg and Khokhlov, 1994), the sharpness of which is augmented by the inflexibility of DNA (Post and Zimm, 1979). Laser light scattering measurements of viral DNA collapse often yield continuous, albeit abrupt, transitions with respect to condensing agent (Benbasat, 1984; Widom and Baldwin, 1980;

Wilson and Bloomfield, 1979). The discrepancy between theory and experiment is thought to arise from competing condensation and aggregation reactions present in solutions not infinitely dilute (Post and Zimm, 1982a,b). Under highly dilute conditions in which overlap of molecular domains is negligible, fluorescence microscopy has been used to follow the collapse of single T4 bacteriophage DNAs induced by multivalent cations (Yoshikawa et al., 1996a,b). These experiments showed that the transition was indeed discontinuous at the single molecule level but continuous for the ensemble average, thus unifying theory and experiment.

The impetus for DNA condensation is generally thought to arise from attractive lateral interactions between adjacent helices generated upon binding a critical amount of multivalent cations. The favorable interactions may reflect the influences of helix hydration (Arscott et al., 1995; Rau and Parsegian, 1992), helix secondary structure (Ma et al., 1995; Reich et al., 1991) and/or electrostatic attraction through ion correlation (Gronbeck-Jensen et al., 1997; Marquet and Houssier, 1991; Oosawa, 1968; Rouzina and Bloomfield, 1996). Manning (1980, 1985), however, has put forth another idea: that sufficiently neutralized DNA will crumple like an overloaded elastic column. This implies that the impetus for collapse arises from the unbalanced retractile force exerted along the backbone of neutralized DNA, rather than from the lateral interactions between helices. In this paper we use manipulations of single DNA molecules, at extensions that preclude intramolecular contacts, to test these competing hypotheses.

In previous work, our two groups, one at Princeton (Wang et al., 1997) and the other a Minnesota-Oregon collaboration (Baumann et al., 1997), used optical tweezers

Received for publication 15 October 1999 and in final form 3 January 2000.

C. Baumann's current address: Department of Biology, University of York, Heslington, York YO10 5DD, United Kingdom.

M. D. Wang's current address: Department of Physics, LASSP, 514 Clark Hall, Cornell University, Ithaca, NY 14853-2501.

S. M. Block's current address: Departments of Biological Sciences and Applied Physics, Herrin Labs 029, Stanford University, Stanford, CA 94305-5020.

Address reprint requests to Victor A. Bloomfield, Department of Biochemistry, University of Minnesota, St. Paul, MN 55108. Tel.: 612-625-2268; Fax: 612-625-6775; E-mail: victor@tc.umn.edu.

© 2000 by the Biophysical Society

0006-3495/00/04/1965/14 \$2.00

to study the effects of cations on the elasticity of single DNA molecules. We used different apparatus and different DNA: a plasmid containing 3888 basepairs (bp) in one case, and  $\lambda$  bacteriophage DNA containing 48,502 bp in the other. However, we obtained very similar results, notably that the trivalent cations spermidine and hexaammine cobalt(III), commonly used as DNA condensing agents, markedly increase the apparent bending flexibility (entropic elasticity) of DNA above the supposed limiting value achieved in high concentrations of monovalent salt. The increased bending is due to asymmetric shielding of the DNA phosphate charge by multivalent ligands (Rouzina and Bloomfield, 1998; Stigter, 1998). The force-extension curves are well fit by a worm-like chain (WLC) model, with a lowered persistence length  $P$  resulting from increased bending flexibility. In those experiments we observed that at low stretching forces and under condensing ionic conditions, individual molecules often deviated from WLC elastic behavior, yielding instead a reversible force plateau which was attributed to intramolecular DNA condensation.

In this paper we report further investigations on the dependence of single molecule condensation on ionic conditions and extent of stretching. We present results from our two groups together in a single paper, despite significant differences in experimental details, so that we and our readers can critically examine the dependence of the results on these details. We find good correlation with the conditions for DNA condensation in solution. We find that intramolecular condensation can occur only when the DNA is sufficiently relaxed that intramolecular loops can occur, providing strong support for a lateral interaction rather than an elastic buckling mechanism. A first-order phase transition explains the discontinuous change in force with extension.

## MATERIALS AND METHODS

### DNA, buffers, and multivalent cation solutions

The Minnesota-Oregon group used  $\lambda$  DNA. The 5'-overhangs of  $\lambda$  DNA (methylated *c1857ind 1 Sam 7*, New England Biolabs, Beverly, MA) were biotinylated with the Klenow *exo*-enzyme (New England Biolabs) using bio-11-dCTP (Sigma, St. Louis, MO), dATP, dGTP, and dUTP as described previously (Smith et al., 1996). Single-strand nicks were repaired with T4 DNA ligase. After biotinylation and nick ligation, DNA stocks were stored in an EDTA-containing buffer.

Monovalent salt buffer solutions were prepared using 100 mM cacodylate, pH 7, buffer stocks (86.2 mM sodium cacodylate, 13.8 mM cacodylic acid) supplemented with either 100 or 500 mM NaCl (total  $\text{Na}^+$  concentration  $\sim 186$  and 586 mM, respectively). Spermidine trihydrochloride (Sigma) and hexaammine cobalt (III) trichloride (Eastman), hereafter abbreviated CoHex, were utilized without further purification and prepared as 0.1-M stocks in deionized water ( $\rho \geq 12 \text{ M}\Omega\text{-cm}$ ). Final experimental solutions were prepared before use by diluting the above buffer and trivalent cation stocks with deionized water. Background buffer (B buffer) is a low ionic strength monovalent buffer, diluted to 1 mM NaCl and 1 mM cacodylate, pH 7; it is typically utilized for bulk condensation studies. Complete buffer exchange between experiments was ensured by monitoring the conductivity of the fluid chamber eluant.

The Princeton group used a 3888-bp DNA molecule, which was PCR-amplified from the plasmid pRL574 as previously described (Wang et al., 1997; Yin et al., 1995). The experimental buffer was  $\text{NaH}_2\text{PO}_4$ , pH 7, containing 10 mM  $\text{Na}^+$  to which various concentrations of spermidine were added.

### Optical trap manipulations of single DNA molecules

In the Oregon apparatus, a biotinylated  $\lambda$  DNA molecule was tethered between two streptavidin-coated polystyrene beads 3.54  $\mu\text{m}$  in diameter (Spherotech, Libertyville, IL). One bead was held by a micropipette (the "micropipette bead") while the other was optically trapped. Two counter-propagating laser beams generated the optical trap within a specially designed fluid chamber, far ( $>100 \mu\text{m}$ ) from the chamber walls. The tension of the DNA molecule was altered by moving the micropipette relative to the trapped bead, and the relative extension determined from the distance between bead centers. The absolute extension was determined by stretching each DNA molecule to the left and right of the trap; this was possible because the trapped bead can rotate and the micropipette bead cannot. The force acting on the molecule was inferred from the displacement of the laser beams on position-sensitive photodetectors, and calibrated against the viscous drag on a bead using Stokes' law (Smith et al., 1996). All single molecule manipulations were conducted within a temperature range of 22.2 to 22.8°C.

The molecule was allowed to equilibrate at each extension for 2 s before averaging the signal at the position detectors for 2 s. At the experimental molecular extensions employed ( $x = 8\text{--}16 \mu\text{m}$ ), the slowest internal normal modes of motion for  $\lambda$  DNA relax in  $<2$  s (Quake et al., 1997). The pause at each extension should thus be sufficient to allow the stretched chain to reach a pseudo-equilibrium. Each force-extension ( $F$ - $x$ ) data point was separated by  $\sim 0.44 \mu\text{m}$ , dictated by the gearing of the stepper motor actuating the micropipette manipulator. The discrete movements of the micropipette subjected the tethered DNA molecule to a stretch/release rate  $<0.22 \mu\text{m/s}$ .

Thermal drift in a dual-beam force transducer is normally reset at zero every few minutes by removing all forces on the trapped particle and nulling the residual signal. In strong condensing solutions, however, some tension must be constantly maintained on the molecule to prevent its premature condensation. In such conditions, the DNA molecule was maintained stretched between trap and pipette along the  $y$  axis, while the force transducer was zeroed along its  $x$  axis. Data were then obtained by pulling the molecule along the  $x$  axis, to both the right and left of the trap. A force plateau was recognized as a constant force acting on the trap bead directly toward the micropipette bead, which simultaneously satisfied the following criteria: it was observed at fractional extensions where the entropic elastic response of  $\lambda$  DNA was expected to be negligible; and it was independent of the spatial orientation (right vs. left) of the micropipette bead relative to the trapped bead.

The elastic response in ionic conditions where DNA condensation is strongly favored was determined by exchanging the sample chamber solution with either 25  $\mu\text{M}$  CoHex or 100  $\mu\text{M}$  spermidine in B buffer. These concentrations are about fourfold higher than required to induce monomolecular condensation of  $\lambda$  DNA in bulk solution (Widom and Baldwin, 1980; Wilson and Bloomfield, 1979). The sample chamber was flushed for 10 to 15 min with the solution of interest, while the molecule was maintained at an extension near its contour length. During the process of tethering a molecule between the two beads, extraneous molecules were often snagged on the beads. Thus, maintaining the primary molecule near full extension prevented unwanted secondary interactions with extraneous molecules during buffer exchange. After complete buffer exchange these molecules collapse and do not interfere with the properly tethered DNA molecule.

In the Princeton apparatus, an optical trapping interferometer, a DNA molecule biotinylated at only one end was tethered between a trapped

avidin-coated polystyrene bead  $0.52 \mu\text{m}$  in diameter (Polysciences, Warrington, PA) and a stalled *Escherichia coli* RNA polymerase complex bound nonspecifically to the microscope coverglass surface (see Yin et al., 1995, for experimental details). Force-extension data were collected as previously described (Wang et al., 1997) with individual molecules stretched/released at a rate  $<0.1 \mu\text{m/s}$  without pausing.

These measurements were performed at a tether density of  $\sim 0.02$  tethers/ $\mu\text{m}^2$ . (In the DNA stretching measurements the tether density was  $<0.003$  tethers/ $\mu\text{m}^2$ .) A tethered bead displayed Brownian motion with a magnitude of  $\sim 1.5 \mu\text{m}$  diameter around its polymerase anchor. The spermidine concentration was raised gradually by flowing the same buffer, with a specific spermidine concentration, through the sample chamber. The extents of Brownian motion of  $N = 16$  tethered beads were examined. As the spermidine concentration increased, an increasing number of tethered beads displayed drastic reductions in their Brownian motions. A DNA molecule was considered to be condensed when its extent of Brownian motion was  $<0.5 \mu\text{m}$  in diameter. The fraction of condensed DNA ( $f$ ) was counted at each spermidine concentration. The error bars were calculated based on the binomial distribution:  $\sqrt{Nf(1-f)}$ .

### Analysis of force-extension curves for WLCs

The WLC model describes the behavior of a DNA molecule as intermediate between a rigid rod and a flexible coil, accounting for both local stiffness and long-range flexibility (Grosberg and Khokhlov, 1994). The flexibility of the chain is described by the persistence length  $P$ , the distance over which two segments of the chain remain directionally correlated. An interpolation formula that describes the extension ( $x$ ) of a WLC with contour length  $L_0$  in response to a stretching force  $F$  is (Bustamante et al., 1994; Marko and Siggia, 1995)

$$\frac{FP}{k_B T} = \frac{1}{4} \left( 1 - \frac{x}{L_0} \right)^{-2} - \frac{1}{4} + \frac{x}{L_0} \quad (1)$$

where  $k_B$  is the Boltzmann constant and  $T$  is the absolute temperature. This equation describes the entropic elasticity of a WLC, arising from the reduced entropy of the stretched chain ( $x/L_0 < 0.97$ ), and assumes the DNA is inextensible. At the high force limit of Eq. 1 ( $x/L_0 = 0.85-0.97$ ),  $x$  approaches  $L_0$  as  $F^{-1/2}$  (Bustamante et al., 1994; Kovac and Crabb, 1982; Marko and Siggia, 1995); thus plots of  $F^{-1/2}$  versus  $x$  yield  $L_0$  upon extrapolation to infinite  $F$ , while  $P$  is extracted from the y-intercept as  $2(P/k_B T)^{1/2}$ . Deviations from this behavior are observed at still higher forces, due to the stretching of the molecule beyond its theoretical (zero force) contour length, a regime termed enthalpic elasticity. This regime can be accounted for by using a stretch modulus as originally proposed by Odjik (1995) and experimentally measured by Smith et al. (1996).

A modification of Eq. 1 that takes into account stretching of the DNA at or slightly beyond full extension is

$$\frac{FP}{k_B T} = \frac{1}{4} \left( 1 - \frac{x}{L_0} + \frac{F}{K_0} \right)^{-2} - \frac{1}{4} + \frac{x}{L_0} - \frac{F}{K_0} \quad (2)$$

where  $K_0$  is the stretch modulus. In general, the Minnesota-Oregon group used Eq. 1 to analyze data on  $\lambda$  DNA, whereas the Princeton group used Eq. 2 to analyze data on plasmid-length DNA. There was little difference in the derived values of  $L_0$  or  $P$  regardless of which equation was used.

For  $F-x$  curves obtained with  $\lambda$  DNA under condensing conditions,  $P$  was extracted from the high force entropic elasticity ( $5 \leq F \leq 15$  pN) of individual  $\lambda$  DNA molecules after replotting the data as  $F^{-1/2}$  vs.  $x$ . At  $F > 5$  pN the replotted data were linear and not affected by the retractile force (see below). At  $F > 15$  pN the replotted data deviated from linearity due to enthalpic elasticity and were omitted from the WLC analysis.

### Laser light scattering

To compare  $\lambda$  DNA condensation behavior in single molecule stretching experiments with those in solution, total intensity laser light scattering measurements were performed in Minnesota with a Lexel model 95-3 argon-ion laser (Lexel Laser, Fremont, CA) operating at a wavelength of 488 nm and a power output of 100 to 200 mW. The laser beam was focused on a cylindrical scattering cell immersed in a thermostatically controlled ( $25^\circ\text{C}$ ) refractive index matching bath. Scattered light was detected with a ITT FW-130 photomultiplier tube, and the photocurrent generated sent to a Brookhaven Instruments model BI-9000AT correlator (Brookhaven Instruments, Holtsville, NY) after pulse amplification and discrimination. The photon counts recorded per second were calibrated using benzene as a reference scatterer. DNA condensation was monitored at a scattering angle of  $90^\circ$  using a  $\lambda$  DNA molecular concentration of  $\sim 3$  pM (corresponding to  $9.5 \times 10^{-5}$  mg/ml).

## RESULTS

### Stretching single DNA molecules under condensing conditions

The  $F-x$  curve of a single  $\lambda$  DNA molecule in the Oregon apparatus under various ionic conditions is plotted in Fig. 1.

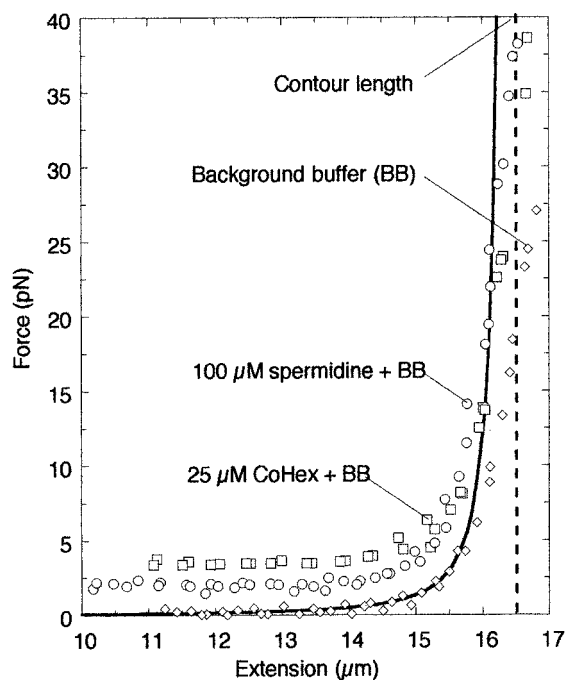


FIGURE 1 Response of single  $\lambda$  DNA molecules to an applied force with condensing concentrations of the trivalent cations CoHex and spermidine. The molecule in the low monovalent salt background buffer ( $\diamond$ ) displayed low and high force entropic elasticity indicative of a WLC with  $P = 95$  nm and  $L_0 = 16.5 \mu\text{m}$  (solid curve). Upon addition of either  $25 \mu\text{M}$  CoHex ( $\square$ ) or  $100 \mu\text{M}$  spermidine ( $\circ$ ) to this low monovalent salt buffer,  $\lambda$  DNA molecules displayed high force elasticity indicative of a WLC with increased chain flexibility ( $P < 50$  nm). Near three-fourths extension ( $x = 13-14 \mu\text{m}$ ), an abrupt loss of WLC behavior occurred, replaced by a force plateau (1-4 pN in magnitude) which was reproducible during both stretch and release cycles. The vertical broken line represents the B form contour length of  $\lambda$  DNA.

The elastic response in B buffer, containing just monovalent cations and thus not causing condensation, yields from the high force limit of Eq. 1 a WLC with a persistence length of 95 nm and a contour length of 16.5  $\mu\text{m}$ , in accord with our previous results (Baumann et al., 1997).

The elastic response was then recorded under ionic conditions where DNA condensation would be strongly favored by addition of trivalent cations (see below). Fig. 1 shows data for molecules in the presence of 25  $\mu\text{M}$  CoHex plus B buffer, and 100  $\mu\text{M}$  spermidine plus B buffer. At nearly full extensions, the  $F$ - $x$  curves rose more rapidly than in monovalent buffer alone as  $x \rightarrow L_0$ , indicating increased flexibility, i.e., a reduced persistence length (12–26 nm for CoHex and 25–38 nm for spermidine, compared with 50 nm for high concentrations of NaCl). The extension was then decreased, and near three-fourths maximal extension ( $x = 13$ –14  $\mu\text{m}$ ), stretched  $\lambda$  DNA molecules abruptly departed from WLC behavior, yielding a retractile force of constant magnitude (1–4 pN). The force remained constant down to the shortest molecular extensions probed ( $x \leq 8 \mu\text{m}$ ). Data were not collected below this extension to prevent potential bead-DNA entanglements under condensing solution conditions. This abrupt departure from WLC behavior was reproducible during both stretch and release cycles.

The Princeton group measured the force-extension relation for plasmid-length DNA molecules at relatively high spermidine concentrations ( $>200 \mu\text{M}$ ), where most of the DNA molecules are condensed and only a small fraction were not condensed. The behavior of plasmid-length DNA with the Princeton apparatus was similar to that of  $\lambda$  DNA in the Oregon apparatus for those molecules that did not condense at a given spermidine concentration.  $F$ - $x$  curves of uncondensed DNA displayed the same characteristics as those measured in the absence of spermidine. Fig. 3 A shows an example of these curves. Data (solid dots) with  $F < 5$  pN were well fit with Eq. 1:  $P = 38.25$  nm and  $L_0 = 1324$  nm. For data with  $F > 5$  pN, a slight deviation from

Eq. 1 can be seen due to the enthalpic elasticity of the DNA molecules at large forces. Fitting the entire  $F$ - $x$  curves according to Eq. 2 yielded the DNA elasticity parameters in Table 1. As the spermidine concentration was increased,  $P$  decreased and reached a plateau. This trend inversely correlates with the fraction of charges neutralized on the DNA backbone (Fig. 2), indicating that the persistence length of DNA decreases with increasing neutralization of the DNA backbone charges.

Force-extension curves were also measured with condensed plasmid-length DNA. Two distinctive types of curves were observed, stick-release and plateau. Eleven of 15 curves showed stick-release patterns (Fig. 3 B), in which the DNA began with a given stiffness and apparent contour length, and then slipped into a different stiffness and contour length. The slip happened frequently (typically 2 to 6 times) during the stretch phase, to a variable degree, usually on the order of 100–150 nm, and with a variable peak force, usually on the order of 5–15 pN. The  $F$ - $x$  curves preceding the four force peaks in Fig. 3 B represent polymers of decreasing stiffness ( $p = 24, 19, 18,$  and 11 nm, from left to right, as calculated from Eq. 2, with the completely stretched polymer possessing a stiffness identical to an uncondensed DNA tether ( $P \approx 40$  nm). The mechanism of this apparent persistence length change is unclear. During the relaxing phase, we observed hysteresis and no stick-release behavior. This phenomenon mimics that of titin (Rief et al., 1997) and tenascin (Oberhauser et al., 1998) stretching, and may correspond to one or more turns of DNA in a coiled, condensed structure being released suddenly during a stick-release. However, the possibility cannot be excluded that they are due instead to the sticking of DNA to either the glass coverslip or the trapped microsphere. A subtle feature of the stick-release pattern is that the maximum force increases with extension. If these peaks represent the unpacking of DNA from a coiled structure, then the liberated DNA regions are sorted by unpacking

**TABLE 1 Measured DNA elastic parameters with various ionic conditions**

Buffer composition	$P$ (nm)	$K_0$ (pN)	$L_0$ (nm)
<b>Plasmid DNA</b>			
10 mM Na <sup>+</sup>	47.4 $\pm$ 1.0 (14)	1008 $\pm$ 38 (10)	1343 $\pm$ 5 (10)
10 mM Na <sup>+</sup> and 10 $\mu\text{M}$ Spd <sup>3+</sup>	40.7 $\pm$ 1.4 (11)	1166 $\pm$ 114 (6)	1335 $\pm$ 5 (6)
10 mM Na <sup>+</sup> and 100 $\mu\text{M}$ Spd <sup>3+</sup>	38.7 $\pm$ 1.0 (8)	1202 $\pm$ 83 (5)	1313 $\pm$ 2 (5)
10 mM Na <sup>+</sup> and 200 $\mu\text{M}$ Spd <sup>3+</sup>	40.6 $\pm$ 1.1 (8)	1253 $\pm$ 13 (3)	1318 $\pm$ 12 (3)
10 mM Na <sup>+</sup> and 300 $\mu\text{M}$ Spd <sup>3+</sup>	38.9 $\pm$ 0.8 (2)	1070 $\pm$ 158 (2)	1333 $\pm$ 11 (2)
<b><math>\lambda</math> DNA</b>			
1.86 mM Na <sup>+</sup>	86.2 $\pm$ 4.9 (7)		16,748 $\pm$ 76 (7)
1.86 mM Na <sup>+</sup> + 25 $\mu\text{M}$ CoHex	14.8 $\pm$ 1.4 (3)	16,909 $\pm$ 133 (3)	
9.3 mM Na <sup>+</sup> + 25 $\mu\text{M}$ CoHex	15.0	16,845	
186 mM Na <sup>+</sup> + 25 $\mu\text{M}$ CoHex	51.5	16,688	
1.86 mM Na <sup>+</sup> + 100 $\mu\text{M}$ Spd <sup>3+</sup>	32.4		16,742
9.3 mM Na <sup>+</sup> + 100 $\mu\text{M}$ Spd <sup>3+</sup>	44.8		16,674
186 mM Na <sup>+</sup> + 100 $\mu\text{M}$ Spd <sup>3+</sup>	48.0		16,621
186 mM Na <sup>+</sup>	54.1 $\pm$ 3.3 (3)		16,745 $\pm$ 82.4 (3)

For cases in which more than one DNA molecule was measured, the table gives mean  $\pm$  SE (number of molecules).

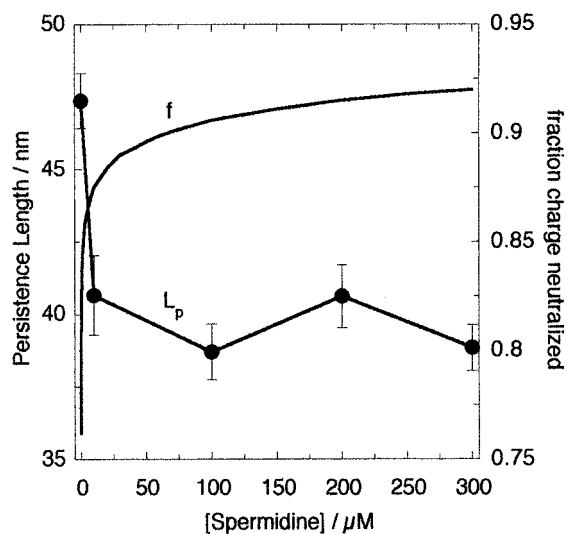


FIGURE 2 Persistence length ( $L_p$ ) as a function of spermidine concentration for single, uncondensed plasmid-length DNA tethers stretched using the Princeton apparatus. This figure illustrates that the persistence length of DNA decreases as the charge on the DNA backbone is neutralized. Fraction of charge neutralized was calculated using counterion condensation theory (Manning, 1978; Wilson and Bloomfield, 1979).

force, rather than position in the DNA chain. This disfavors desorption from a surface as the explanation for the stick-release pattern, but it also implies that the condensed plasmid forms several independent condensed globules aligned in series.

In four of 15 curves, force-extension curves with a plateau were observed. Fig. 3 C shows a plateau at  $\sim 20$  pN of force that was present during both the stretch and release. The plateaus are reminiscent of the overstretching behavior of DNA (Smith et al., 1996). This plateau may be due to an interaction between two or more condensed DNA tethers, i.e., multiple, overlapping stick-release patterns lead to force plateau, as was observed when multiple spectrin tethers were unfolded by stretching (see Fig. 4 of Rief et al., 1999).

### Dependence of single molecule condensation on ionic conditions

If the force plateau arises because of intramolecular DNA condensation, then the same sensitivity to counterion valence and monovalent ionic strength should be observed as is seen in bulk condensation. As a first test, neither  $100 \mu\text{M Mg}^{2+}$  nor  $100$  and  $200 \mu\text{M putrescine}^{2+}$  induced a force plateau with  $\lambda$  DNA at low molecular extensions, although approximately twofold decreases in persistence length were observed (Baumann et al., 1997). Thus divalent cations cannot induce a force plateau, just as they cannot induce bulk DNA condensation in aqueous solution (Widom and Baldwin, 1980; Wilson and Bloomfield, 1979).

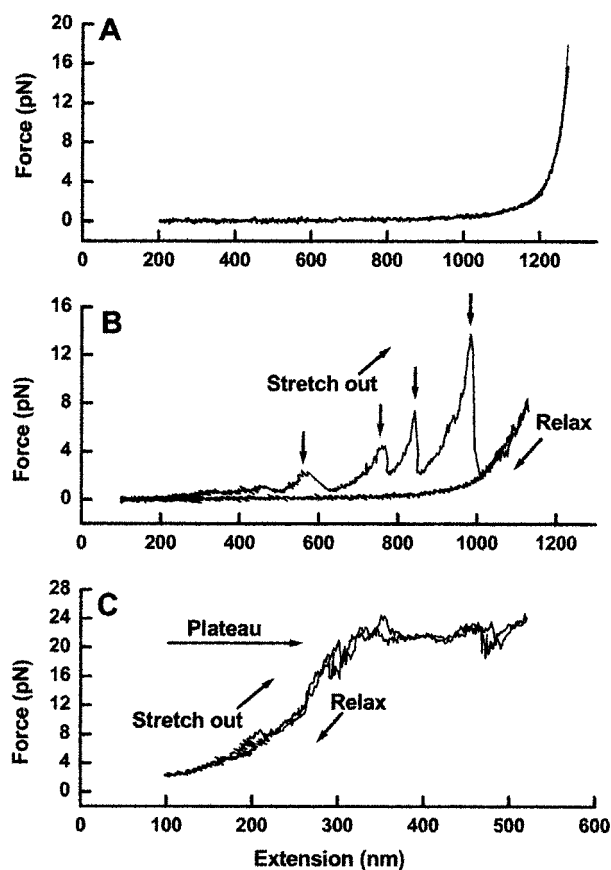


FIGURE 3 Stretching plasmid-length DNA tethers at condensing conditions where the  $[\text{spermidine}] > 200 \mu\text{M}$ . (A) Uncondensed molecules displayed force-extension curves characteristic of a worm-like chain. Data at  $F < 5$  pN was well fit by Eq. 1, yielding  $P = 38.25$  nm and  $L_o = 1324$  nm (solid line). Force-extension curves for condensed DNA molecules showed two distinct behaviors. (B) Most of the curves showed a stick-release pattern. Here the DNA molecule begins with a given stiffness and apparent contour length, and slips into a different stiffness and contour length, with a variable degree of slip (100–150 nm). The  $F$ - $x$  curves preceding the four force peaks represent polymers of decreasing stiffness ( $P = 24, 19, 18,$  and  $11$  nm from left to right), with the completely stretched polymer possessing a stiffness identical to an uncondensed DNA tether ( $P = 40$  nm). During the relaxing phase, the DNA shows no stick-release behavior, but the  $F$ - $x$  curve displays hysteresis. (C) A few DNA tethers show a force plateau behavior during both stretch and release. The  $F$ - $x$  curve displays a plateau ( $\sim 20$  pN) where little or no additional force is required for increased extension.

To determine if the observed force plateau was sensitive to monovalent ionic strength, the elastic response of  $\lambda$  DNA in  $25 \mu\text{M CoHex}$  (Fig. 4) and  $100 \mu\text{M spermidine}$  (Fig. 5) was measured as a function of NaCl concentration and plotted as  $F^{-1/2}$  versus fractional extension ( $y = x/L_o$ ) according to Eq. 1.  $F$ - $x$  data plotted in this manner highlight both the dependence of the force plateau on NaCl concentration and the high force WLC entropic elasticity from which the persistence length was extracted (Baumann et al., 1997). Individual molecules abruptly deviated from WLC behavior at fractional extensions  $< 0.85$  for NaCl concen-

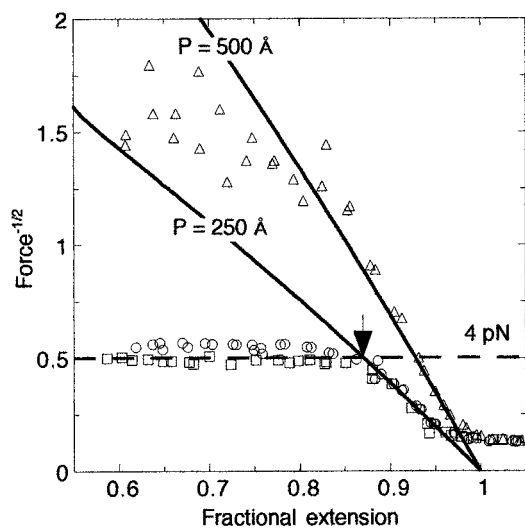


FIGURE 4 Effect of monovalent salt on the entropic elasticity of single  $\lambda$  DNA molecules in  $25 \mu\text{M}$  CoHex. At  $[\text{NaCl}] = 1$  ( $\circ$ ) or  $5$  mM ( $\square$ ) and fractional extensions ( $0.85$ ,  $\lambda$  DNA displayed an abrupt loss of WLC elasticity (*arrow*). Below this extension, a force plateau ( $\sim 4$  pN) was observed during stretch and release cycles (*dashed line*). At fractional extensions  $>0.85$  these molecules displayed WLC behavior consistent with a decreased persistence length ( $P$ ). The plateau was not observed with  $[\text{NaCl}] = 186$  mM ( $\triangle$ ); instead, the expected high monovalent salt WLC behavior was obtained at low extensions. The entropic elastic response of WLC (*solid lines*) with  $P = 25$  and  $50$  nm are provided as a comparison.

trations of  $1$  and  $5$  mM. The force plateau below this extension was constant in magnitude and reproducible during both stretch and release cycles. As the NaCl concentration was increased at a constant CoHex or spermidine concentration, the force plateau disappeared and the expected low force WLC entropic elasticity returned, as described below.

### Magnitude of condensation force

The magnitude of the force plateau depended on the trivalent cation utilized, with strongly condensing concentrations of CoHex yielding a higher maximum force ( $\sim 4$  pN) than spermidine ( $\sim 1$  pN). If the force plateau seen at fractional extensions  $<0.85$  is associated with DNA condensation, the plateau presumably represents the force  $F_r$  required to convert condensed regions of the DNA chain to an extended form. The work  $W$  done during a change in DNA extension of magnitude  $\Delta x$  from  $x_1$  to  $x_2$  is

$$W = \int_{x_1}^{x_2} F dx = F_r \Delta x \quad (3)$$

This yields  $W \approx 0.083$   $kT/\text{bp}$  for spermidine and  $W \approx 0.33$   $kT/\text{bp}$  for CoHex, assuming a B-helix rise per bp of  $0.338$  nm (Saenger, 1984) and  $\Delta x = 0.44 \mu\text{m}$  (the length of DNA released or condensed during a change in extension for the

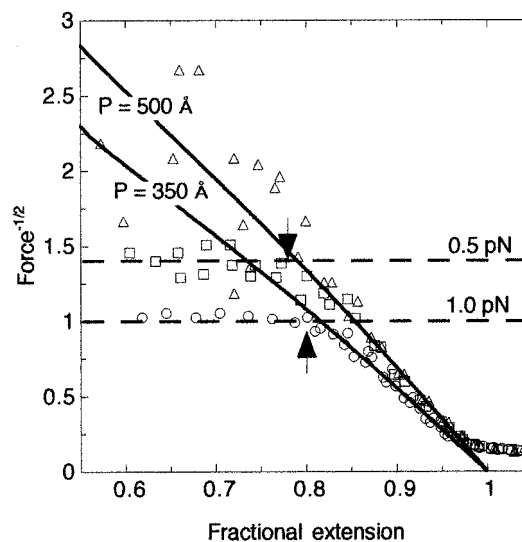


FIGURE 5 Effect of monovalent salt on the entropic elasticity of single  $\lambda$  DNA molecules in  $100 \mu\text{M}$  spermidine. At  $[\text{NaCl}] = 1$  ( $\circ$ ) or  $5$  mM ( $\square$ ) and fractional extensions ( $0.8$ ,  $\lambda$  DNA displayed an abrupt loss of WLC elasticity (*arrows*). Below this extension, a force plateau ( $0.5$ – $1$  pN) was observed during stretch and release cycles (*dashed lines*). At fractional extensions  $>0.8$ , these molecules displayed WLC behavior consistent with a decreased persistence length  $P$ . The plateau was not observed with  $[\text{NaCl}] = 186$  mM ( $\triangle$ ), instead the expected high monovalent salt WLC behavior was obtained at low extensions. The entropic elastic response of WLC (*solid lines*) with  $P = 35$  and  $50$  nm are provided as a comparison.

Oregon apparatus). These values of  $W$  are in reasonable accord with osmotic pressure-volume measurements of the intermolecular force provoked by CoHex in bulk condensed DNA ( $-0.17$   $kT/\text{bp}$ ; Rau and Parsegian, 1992), and with theoretical estimates of the attraction due to correlated ion fluctuations of bound counterions ( $-0.34$   $kT/\text{bp}$ ; Marquet and Houssier, 1991) and hydration forces ( $-0.12$   $kT/\text{bp}$ ; Bloomfield, 1991) in condensed DNA.

### Correlation of chain flexibility and appearance of force plateau

If intramolecular side-by-side segment contacts are required for the collapse of a stretched DNA chain, then collapse is predicted to correlate with the first short-range intramolecular contacts, i.e., the first intramolecular loops. By definition, a fully stretched chain cannot loop back on itself, and the probability of intramolecular contacts in a somewhat relaxed chain will increase both with decreasing relative extension and with increasing chain flexibility. For a given chain, flexibility increases with the number of statistical segments in that chain, e.g., the number of persistence lengths in a WLC. Thus, one would expect that the fractional extension at which a molecule deviates from WLC behavior ( $y_{\text{crit}}$ ) increases with the number of persistence lengths in the chain (equivalent to  $L_0$  divided by  $P$  for each chain). Values of  $y_{\text{crit}}$  were obtained by comparing experi-

mental  $F$ - $x$  curves with calculated curves for an ideal WLC generated using Eq. 1 with  $P$  extracted from the high force entropic elasticity. In Fig. 6 are plotted the number of persistence lengths in each DNA chain versus  $y_{\text{crit}}$  for several  $\lambda$  DNA molecules displaying a force plateau. As expected, there is a strong correlation ( $r = 0.95$ ). Thus chain flexibility influences the onset of the force plateau, consistent with a requirement for short-range segment-segment interactions in a DNA molecule before intramolecular collapse. The values of  $y_{\text{crit}}$  in CoHex are consistently larger than those in spermidine, showing that stretched DNA chains collapse at larger extensions in CoHex, i.e., require less molecular slack. This is consistent with the greater  $F_r$  measured in CoHex.

Under ionic conditions that would normally cause condensation, but at fractional extensions  $>0.85$  at which side-by-side interactions are unlikely,  $\lambda$  DNA molecules displayed entropic elasticity indicative of a WLC, with  $y \rightarrow 1$  as  $F^{-1/2}$  as shown in Fig. 4 for 25  $\mu\text{M}$  CoHex and in Fig. 5 for 100  $\mu\text{M}$  spermidine. Significant changes in the high force entropic elasticity of  $\lambda$  DNA, as manifested in the persistence length, were induced by varying the NaCl concentration (Table 1). In 1 mM NaCl, persistence lengths were considerably above the high monovalent salt limit of  $\sim 50$  nm (Hagerman, 1988). As [NaCl] was increased, the persistence lengths approached that limit, indicating competitive binding between the multivalent and monovalent counterions at the highly charged surface of DNA. Whether or not the force plateau appears does not depend on increases in chain flexibility, i.e., decreases in the persistence length. However, the extension at which the abrupt separ-

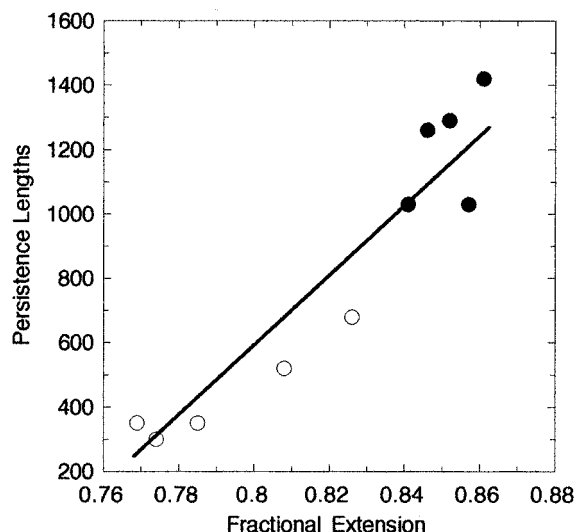


FIGURE 6 Correlation between the number of persistence lengths in stretched  $\lambda$  DNA molecules and the fractional extension at which the force plateau arises. A linear correlation coefficient = 0.95 was obtained for all data obtained in the presence of 25  $\mu\text{M}$  CoHex (●) and 100  $\mu\text{M}$  spermidine (○).

ture from WLC behavior occurs is correlated with increased chain flexibility, i.e., increases in the number of persistence lengths (Fig. 6).

In the Appendix we develop a theoretical treatment of intramolecular looping in a polymer chain under tension. It shows that significant intramolecular contacts can be formed only when the chain is no more than 75–80% extended, in reasonable agreement with our experimental results. While the argument is developed for a random coil rather than a WLC, the conclusions should be similar for a long WLC, such as  $\lambda$  DNA, that contains many persistence lengths.

### Bulk measurements of DNA condensation

Total intensity laser light scattering measurements of  $\lambda$  DNA condensation were conducted under ionic conditions identical to the single molecule stretching experiments, to determine if the conditions for occurrence of the force plateau were the same as those for collapse in bulk solution. The increase in scattering intensity indicative of DNA condensation, i.e., excess scattering above uncondensed  $\lambda$  DNA in low monovalent salt buffer, observed in both 25  $\mu\text{M}$  CoHex and 100  $\mu\text{M}$  spermidine (Fig. 7 A) correlates perfectly with the appearance of the force plateau in single molecule experiments (Fig. 7 B) as the ionic composition is varied. Increases in scattered intensity are consistent with the conversion of individual  $\lambda$  DNA chains from a weakly scattering coil state to a strongly scattering condensed particle with a radius  $\approx 50$  nm. The presence of toroidal particles with this size in the condensed samples was verified using transmission electron microscopy (data not shown).

These results strongly suggest that the force plateau at low extensions is attributable to intramolecular DNA condensation. However, at neutral pH, the streptavidin-coated polystyrene beads (SPB) tethered at the ends of  $\lambda$  DNA are negatively charged (streptavidin  $\text{pI} = 5$ ); thus, the plateau could arise from nonspecific interactions between SPB and  $\lambda$  DNA mediated by bound trivalent cations. This possibility was explored by cocondensing mixtures of SPB ( $\sim 0.034$  pM) and unbiotinylated  $\lambda$  DNA ( $\sim 3$  pM) using both 25  $\mu\text{M}$  CoHex and 100  $\mu\text{M}$  spermidine in B buffer. The reactive SPB surface area available to  $\lambda$  DNA under these conditions is  $\sim 400$ -fold larger than the total DNA surface area, assuming all surfaces are uniformly reactive. After incubation for 4 to 24 h at 25°C, the SPB were selectively pelleted by centrifugation ( $7740 \times g$ ) and the extent of DNA collapse measured using laser light scattering as described above. The scattering intensity after centrifugation was nearly identical to controls without added SPB, indicating that the trivalent cations do not mediate nonspecific interactions between SPB and DNA. Therefore the force plateau can not be attributed to strong nonspecific bead-DNA interactions under condensing solution conditions.

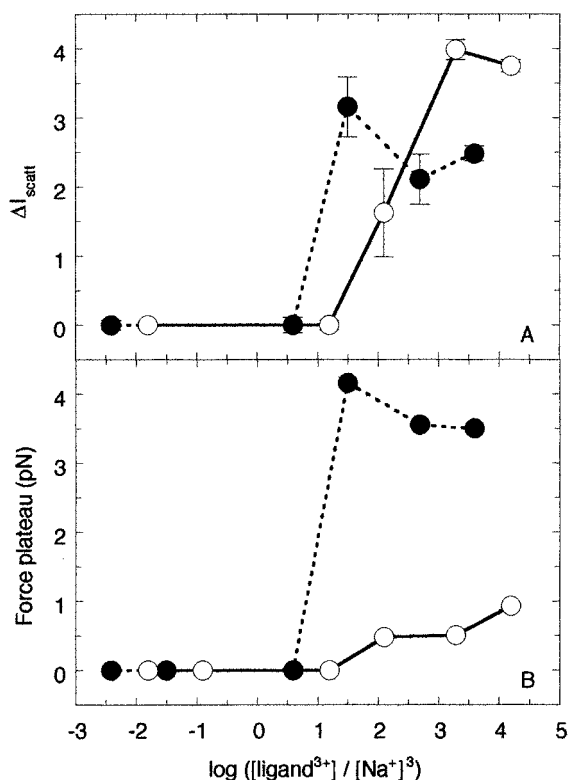


FIGURE 7 Dependence of laser light scattering intensity and retractile force on NaCl concentration with 25  $\mu\text{M}$  CoHex (●) and 100  $\mu\text{M}$  spermidine (○). The NaCl concentration was varied at fixed trivalent cation concentration, and plotted as the  $\log([\text{trivalent ligand}]/[\text{Na}^+]^3)$ . (A) The increases in laser light scattering intensity ( $\Delta I_{\text{scattered}}$ ) observed with CoHex and spermidine are consistent with the transition of  $\lambda$  DNA from a weakly scattering coil to a strongly scattering collapsed particle. Error bars represent the standard deviation of three measurements. (B) The force plateau, observed as a retractile force, at fractional extensions (0.6) is plotted as a function of NaCl concentration. Increases in  $\Delta I_{\text{scattered}}$  coincide with the appearance of the force plateau in single DNA molecules.

Similar results connecting single-molecule and bulk condensation were obtained with plasmid-length DNA tethers (Fig. 8). As the spermidine concentration was increased, the fraction of condensed DNA, as measured by the Brownian motion of the tethered molecules, also increased. The critical concentration for condensation was around 200  $\mu\text{M}$  under the buffer conditions used. This critical concentration is very similar to what has been observed with light scattering measurements under similar buffer conditions.

## DISCUSSION

### Comparison of results from the two laboratories

Results from both of our groups, with different DNA samples, buffers, and instrumentation, show both similarities and differences. The similarities are strong with regard to dependence of persistence length on ionic strength and multivalent ion content (Table 1). The persistence lengths

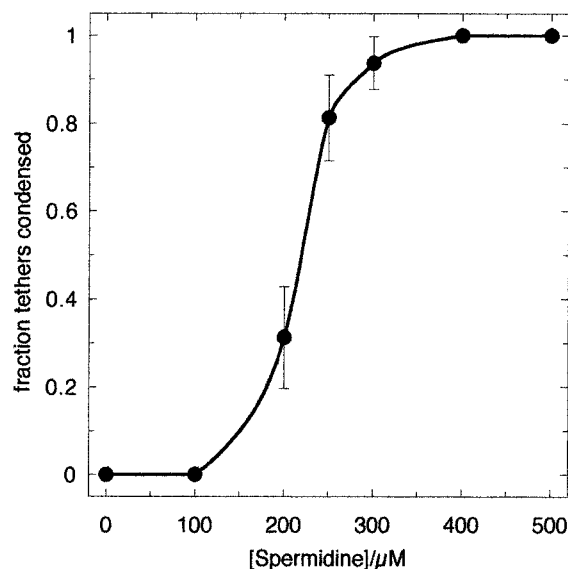


FIGURE 8 Condensation of DNA tethers in the presence of spermidine. This graph plots the fraction of DNA condensed as a function of the spermidine concentration added to the 10 mM  $\text{NaH}_2\text{PO}_4$ , pH 7 buffer. It demonstrates that DNA tethers condense at a spermidine concentration of  $\sim 200$  mM.

measured in 10 mM NaCl are very similar, and both groups observe similar decreases in  $P$  with added  $\text{Mg}^{2+}$  and spermidine<sup>3+</sup>.

The observations are rather different with regard to the force-extension behavior that is observed when relaxed DNA molecules are subject to ionic conditions that cause DNA condensation. The Minnesota-Oregon group observed a constant force plateau at 1 to 4 pN during both the stretching and relaxing cycles under condensing solution conditions, whereas the Princeton group observed stick-slip behavior with a plateau near 20 pN. Both groups agree that the reversible, constant force behavior is most likely to represent the "pure" behavior relevant to DNA condensation. However, the collapsed tethers in the Princeton assays seem to have some kind of structure that could be the target of future investigations.

### Collapse is the result of lateral interactions, not elastic buckling

The trivalent cations CoHex and spermidine strongly influence the elasticity of individual DNA molecules. At high forces and extensions, the entropic elasticity of individual molecules was characteristic of a WLC with a persistence length two- to fourfold less than in the background low monovalent salt buffer. As forces and extensions are lowered, under conditions favoring condensation in bulk, individual DNA molecules deviate abruptly from WLC behavior. Below this point a force plateau of constant magnitude

is observed with  $\lambda$  DNA, which is reproduced during both stretch and release cycles.

We postulate that the force plateau induced by these cations arises from intramolecular DNA condensation. The following observations buttress this interpretation: (i) the plateau occurs in the presence of the trivalent cations CoHex<sup>3+</sup> and spermidine<sup>3+</sup>, known condensing agents in aqueous solution (Widom and Baldwin, 1980; Wilson and Bloomfield, 1979), but not with the divalent cations Mg<sup>2+</sup> and putrescine<sup>2+</sup>, even though these ions reduce the persistence length (which would seem equivalent to elastic buckling); (ii) the ionic conditions required to induce the force plateau are consistent with those needed to induce a critical degree of charge neutralization before DNA condensation (Wilson and Bloomfield, 1979); and (iii) light scattering increases that accompany DNA condensation in bulk solution coincide with a loss of WLC behavior and the appearance of the force plateau in single molecule experiments.

A buckling theory, based on elastic theory for macroscopic rods, predicts that the intrinsic elastic instability of neutralized DNA drives collapse (Manning, 1980, 1985). In this model, stable lateral contacts are a consequence of buckling, rather than the source of nucleation as proposed below. If lateral contacts are not required for collapse, the buckling should manifest itself in stretched DNA molecules at or near their contour length, where lateral contacts can not occur. This does not occur in our experiments. Furthermore, the polyelectrolyte force that prevents buckling is predicted to vary roughly as the logarithm of added monovalent salt at a constant trivalent cation concentration. If our force plateau were due to buckling it should display a similar dependence on monovalent salt. This dependence is not observed (see Fig. 7 B). Instead, there is an abrupt transition when a critical total charge neutralization of the DNA is reached as calculated according to counterion condensation theory (Manning, 1978; Wilson and Bloomfield, 1979). The experimental results obtained here argue against buckling as the source of DNA condensation.

An alternate theory (Halperin and Zhulina, 1991) describing the  $F$ - $x$  response of a single polymer chain in a poor solvent predicts that intramolecular collapse will occur only in the presence of appreciable lateral contacts. Solution conditions favoring DNA condensation can be thought of as poor solvent conditions for DNA. At a fixed extension, the probability of short-range lateral contacts or loop formation will increase with increases in chain flexibility (decreases in the persistence length of a WLC). We observe that the exact extension where the loss of WLC elasticity occurs is proportional to chain flexibility (inversely proportional to the persistence length). This strongly suggests that the loss of WLC behavior requires intramolecular contacts.

According to the above theory (Halperin and Zhulina, 1991), a stretched polymer chain in a poor solvent will collapse when the attractive free energy favoring collapse exceeds the free energy of the stretched polymer, leading to

a first-order phase transition. The transition is observed as a discontinuous change in force with extension, representing a regime where collapsed and uncollapsed regions of the chain coexist. The force plateau observed in the elastic response of single DNA molecules under condensing solution conditions exactly follows this predicted behavior. First-order behavior implies that collapse is nucleation-limited (i.e., requires formation of a nucleus of attractively interacting segments), which in turn stipulates lateral contacts. This interpretation is in complete agreement with recent fluorescence microscopy experiments, where the first-order intramolecular collapse of single viral DNA molecules was observed in the presence of multivalent cations (Yoshikawa et al., 1996a,b).

The theoretical work of Post and Zimm (1979) dealt with the contributions of both chain flexibility and favorable segment-segment interactions to monomolecular DNA collapse. Using Flory-Huggins polymer lattice theory, they predicted that collapse would involve a first-order transition at a critical segment density (dependent on  $P$ ) and  $\chi$ , the Flory polymer-solvent interaction parameter (Post and Zimm, 1979). For a more flexible chain (shorter persistence length), the discontinuous change in polymer volume accompanying collapse occurs at a lower value of  $\chi$  (lower cation concentration). These predictions are in good agreement with the putative first-order transition seen here in single  $\lambda$  DNA molecules, and the four- to sixfold efficiency of CoHex over isovalent spermidine as a condensing agent in bulk solution (Benbasat, 1984; Thomas and Bloomfield, 1983; Widom and Baldwin, 1980).

### Nucleation of intramolecular collapse in a stretched DNA chain

The solution conditions favoring DNA condensation may be thought of as a poor solvent for DNA, one in which segment-segment interactions are favored over segment-solvent interactions. The  $F$ - $x$  response of a single stretched polymer chain in a poor solvent has been treated theoretically (Halperin and Zhulina, 1991). Three deformation regimes are predicted as a function of extension, due to an interplay of the entropic elasticity of the uncollapsed chain and the surface energy of the collapsed globule. First (regime I), at low extensions (extension less than the radius of collapsed globule), the collapsed globule is weakly perturbed by increases in extension. At intermediate extensions (regime II), collapsed and uncollapsed regions of chain coexist and the force is predicted to be roughly independent of changes in extension. At large extensions (regime III), the intrinsic entropic elasticity of the stretched chain is observed. The extension at which the elastic behavior interconverts between regimes II and III is that at which the repulsive force acting on the stretched polymer chain balances the attractive force favoring collapse. If stretching occurs continuously, this  $F$ - $x$  behavior resembles a first-

order transition, such as that between a gas and a liquid, with extension analogous to volume and force to temperature. In our work, regime II would coincide with the extensions where the force plateau is observed, and regime III would represent the high force WLC elasticity.

Our model for such a first-order transition in a stretched  $\lambda$  DNA molecule is presented in Fig. 9. In regime III (Fig. 9 A), the elastic free energy of the stretched chain ( $G_{wlc}$ ) exceeds the magnitude of the net attractive (negative) free energy favoring nucleation of the condensed phase ( $G_{nuc}$ ). At these extensions thermal motion may create temporary slack, enabling loops to form and side-by-side association to occur; however, the collapsed nuclei formed would be unstable. At the boundary between regimes II and III (Fig. 9 B),  $-G_{nuc} \geq G_{wlc}$  and collapse would occur via a stable nucleus, consuming all available molecular slack. The molecular slack present when the force plateau arises is roughly equivalent to the length of DNA ( $L$ ) required to nucleate collapse in the stretched chain ( $L/L_0 = 1 - y_{crit}$ ). In regime II (Fig. 9 C), molecular slack generated would coalesce with the condensed phase. At these extensions collapsed and uncollapsed regions of the chain coexist: the metastable DNA chain is caught in the middle of a phase transition. Below we estimate the magnitude of  $G_{nuc}$  in order to predict the extension at which intramolecular collapse will occur, i.e., the extension where WLC behavior is lost.

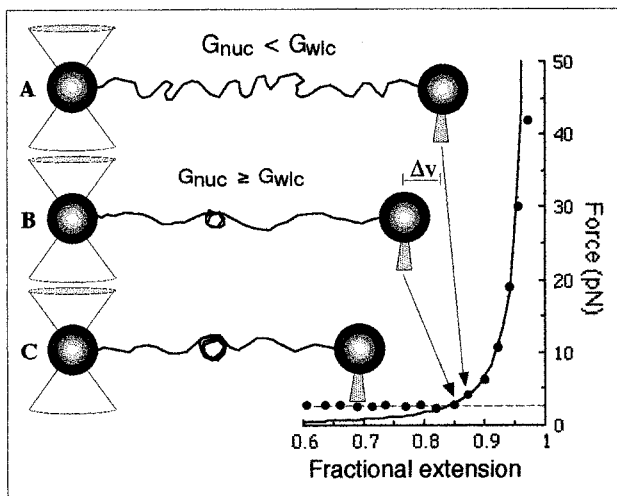


FIGURE 9 Model for a first-order transition in a  $\lambda$  DNA molecule constrained by force-measuring optical tweezers. (A) At fractional extensions  $y > y_{crit}$ , the free energy of the stretched DNA chain ( $G_{wlc}$ ) exceeds the nucleation energy for collapse ( $G_{nuc}$ ). (B) At  $y = y_{crit}$ , characteristic high force WLC elasticity (solid line) is lost;  $G_{nuc}$  overcomes  $G_{wlc}$  and collapse occurs via a stable nucleus consuming all available molecular slack. (C) At  $y < y_{crit}$ , molecular slack generated coalesces into the condensed phase. The force plateau at  $y < y_{crit}$  (dashed line) represents the work required to remove the condensed higher order structure from the DNA chain. For the  $F$ - $x$  data plotted,  $y_{crit} = 0.85$ . This diagram is not drawn to scale.

$G_{nuc}$  must overcome  $G_{wlc}$  if collapse is to occur in a stretched DNA chain. The high force elasticity of  $\lambda$  DNA is well described by a WLC model; therefore, we assume the free energy of  $\lambda$  DNA when stretched is equivalent to that of a WLC, given by (Bustamante et al., 1994)

$$\frac{G_{wlc}(y)}{kT} = \frac{L_0}{P} \left[ \frac{y^2}{2} - \frac{y}{4} + \frac{1}{4(1-y)} - \frac{1}{4} \right] \quad (4)$$

$G_{nuc}$  represents a sum of both repulsive (bending, mixing, and electrostatic forces) and attractive (ion correlation, helix secondary structure perturbations, and hydration forces) contributions. Upon collapse, the bending free energy

$$\frac{G_b}{kT} = \frac{LP}{2r_c^2} \quad (5)$$

and the mixing free energy

$$\frac{G_m}{kT} = \frac{L}{P} \quad (6)$$

would make positive contributions to  $G_{nuc}$ . Here  $L$  is the length of DNA involved in nucleation and  $r_c$  is the radius of curvature for a toroidal nucleus. The residual unscreened charge of DNA will repel neighboring segments and will also contribute a positive free energy ( $G_e$ ) to collapse.  $G_e$  was estimated previously to be  $\sim 0.06$   $kT/bp$  using two parallel polyanionic rods with 89% of their charge neutralized by counterion condensation to represent condensed DNA (Bloomfield, 1991). In order to estimate the extension at which  $\lambda$  DNA will deviate from WLC behavior, the following assumptions are made: (i) the critical radius of the toroidal collapse nucleus is assumed equivalent to the persistence length ( $r_c \approx P$ ). This is consistent with our previous experimental observations (Plum et al., 1990); and (ii) the attractive component of  $G_{nuc}$  ( $G_a$ ) is assumed equivalent to  $L$  multiplied by  $-W$  (Eq. 3), where  $W \approx 0.1$   $kT/bp$  for spermidine and  $\approx 0.3$   $kT/bp$  for CoHex.

The values of  $G_{nuc}$  obtained as a sum of  $G_b$ ,  $G_m$ ,  $G_e$ , and  $G_a$  are tabulated in Table 2 for 25  $\mu M$  CoHex and 100  $\mu M$  spermidine in 1 mM NaCl. We observe that the calculated values of  $G_{nuc} \approx G_{wlc}$  at the fractional extension where the force plateau arises in our experiments. The free energy of a stretched WLC (Eq. 3), calculated for  $P = 17$  and 40 nm, is plotted in Fig. 10 as a function of fractional extension. Calculated data points represent  $G_{nuc}$  from Table 2 for  $\lambda$  DNA molecules displaying a reproducible force plateau in 25  $\mu M$  CoHex and 100  $\mu M$  spermidine. Extrapolation to the  $x$  axis yields  $y_{crit}$  values identical to those observed experimentally. These estimates show that the molecular slack present at fractional extensions  $= y_{crit}$  is consistent with the length of DNA required to nucleate collapse in a stretched DNA chain.

**TABLE 2** Thermodynamic contributions to intramolecular collapse in a stretched DNA molecule

Condition	Solution							
	$L$ (bp)*	$P$ (nm)	$G_v/kT$	$G_m/kT$	$G_e/kT$	$G_a/kT$	$G_{nuc}/kT$	$G_{wlc}/kT^\dagger$
25 $\mu$ M CoHex	7280	17	73	146	437	-2184	-1528	1520
100 $\mu$ M spermidine	12100	40	52	103	726	-1210	-329	348

\* $L = (1 - y_{crit}) (48,502 \text{ bp})$ .

$^\dagger$ Calculated using Eq. 4.

### Differences between CoHex and spermidine

We have shown that a simple nucleation model for intramolecular collapse in a stretched DNA chain, incorporating appropriate attraction and repulsion terms, is sufficient to explain the magnitude of the force plateau and the critical extension where WLC behavior is lost (Fig. 7). Deviation from WLC behavior occurs at larger extensions with condensing concentrations of CoHex than with spermidine. We interpret this to mean that the critical number of interactions between base pairs that is required to nucleate collapse in a stretched DNA chain is less with CoHex. The requirement for a smaller nucleus with CoHex as the condensing counterion may be a result of the larger reduction in the persistence length. This reduction would decrease the volume occupied by the DNA molecule, thus increasing the local concentration of DNA segments and the probability of intramolecular contacts through a reduction in search space.

The force plateau observed with CoHex is consistently greater than that seen with spermidine. This implies that the strength of the intramolecular forces within CoHex-condensed DNA is also larger by an equivalent amount. Per-

haps the more stable interstrand forces we observe in single DNA molecules condensed by CoHex also contribute to the efficiency of this ion as a condensing agent. However, osmotic stress measurements with spermidine and CoHex suggest that these ions induce similar intermolecular forces (interpreted as hydration forces) in bulk condensed DNA (Rau and Parsegian, 1992). Because the two cations bind to DNA with similar affinity and monovalent salt dependence (Braunlin et al., 1982; Plum and Bloomfield, 1988), the differences must reflect ion-specific effects on ion correlation and/or local DNA secondary structure. Furthermore, the forces driving collapse in a single DNA chain may include additional influences which are not observed, or contribute only weakly, to the stabilization of bulk condensed DNA. Intramolecular looping might be one such influence.

### Free polymer ends not required for collapse

A tethered DNA molecule is analogous to a chain without free ends. Theory predicts that nucleation of collapse in a single heteropolymer such as DNA will proceed from an end (Ostrovsky and Bar-Yam, 1995). Our results show that polymer ends are not required for intramolecular DNA collapse. Nucleation in a stretched chain probably involves DNA looping to form the necessary lateral contacts required to initiate collapse. This does not speak to the question of whether collapse from an end is favored in unconstrained linear polymers, although some results from our laboratory (Schnell et al., 1998) suggest that this is the case.

### Implications for biological processes involving DNA unpackaging

The unspooling of condensed DNA by piconewton forces may have important implications for the energetics of biological processes involving DNA unpackaging. For example, research on chromatin loops suggests that transcription involves the sliding of template DNA past immobilized RNA polymerase molecules (Cook, 1994). We observe that the mechanical force required to decondense DNA (<5 pN) is smaller in magnitude than the stalling force of single RNA polymerase molecules (~13 pN; Yin et al., 1995). If we assume that the forces stabilizing multivalent cation-condensed and nucleosome-packaged DNA are similar,

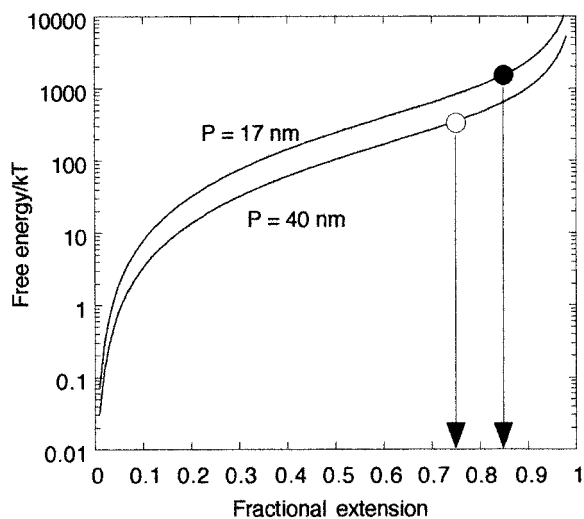


**FIGURE 10** Free energy of a stretched WLC as a function of fractional extension. The curves were calculated with Eq. 3 for persistence lengths  $P = 17$  and  $40$  nm. Calculated data points represent  $G_{nuc}$  from Table 1 for  $\lambda$  DNA molecules displaying a reproducible force plateau in  $25 \mu\text{M}$  CoHex (●) and  $100 \mu\text{M}$  spermidine (○). Extrapolation to the  $x$  axis yields  $y_{crit}$  values identical to those observed experimentally.

then perhaps immobilized processive enzymes generate sufficient mechanical force in vivo to unpackage downstream nucleosomal DNA, thus enabling processing of the DNA template.

## SUMMARY

Our results provide the following new information about intramolecular DNA condensation: (i) intramolecular DNA collapse proceeds via a nucleation-limited mechanism that does not require free polymer chain ends; (ii) Approximately half as many basepairs are required to nucleate collapse in a stretched DNA chain when CoHex, rather than spermidine, is the condensing agent; and (iii) The forces stabilizing DNA collapse are not equivalent for the isoivalent cations CoHex and spermidine. The larger attractive force seen with CoHex may explain the efficiency of this ion as a condensing agent.

## APPENDIX: Probability of loop formation in stretched polymer chain

We assume that the region of DNA extensions in which the force is unvarying, but non-zero, represents the region in which short-range interactions between segments of the same DNA molecule can occur. We investigate whether this is consistent with theoretical expectation by calculating the conditions under which loops in a highly stretched chain can occur with significant probability.

We begin with the familiar treatment of a stretched, freely jointed polymer chain (Flory, 1953; James and Guth, 1943) in which the end-to-end extension  $\bar{x}$  in the direction of a force  $\tau$  is

$$\bar{x} = nL\left(\frac{l\tau}{k_B T}\right) \quad (\text{A1})$$

where  $n$  is the number of statistical segments in the chain, each of length  $l$ , and  $L(\cdot)$  is the Langevin function. The force needed to maintain a given extension is then

$$\tau = \frac{k_B T}{lL^*(x/nl)} \quad (\text{A2})$$

where  $L^*$  is the inverse Langevin function. Each segment in the chain is subject to this force.

We now simplify the problem in two respects, neither of which is likely to affect the qualitative validity of the results. We assume that the stretched chain is effectively one-dimensional, and we assume that each segment can assume only two orientations, either parallel or antiparallel to the force. The probability of the parallel orientation is

$$p = A \exp\left(\frac{l\tau}{k_B T}\right) = A \exp\left[L^*\left(\frac{\bar{x}}{nl}\right)\right] = A \exp[L^*(y)] \quad (\text{A3})$$

where  $y$  is the relative extension and the normalization factor is

$$A^{-1} = \exp\left(\frac{l\tau}{k_B T}\right) + \exp\left(-\frac{l\tau}{k_B T}\right) \quad (\text{A4})$$

The probability of the antiparallel orientation is

$$q = 1 - p. \quad (\text{A5})$$

The binomial distribution  $P(m, k; p)$  gives the number of ways in which  $k$  states occurring with probability  $p$  can be chosen from  $m$  total states. In order for a sequence of  $m$  segments within the stretched chain to form a loop, the number of parallel and antiparallel orientations must be equal to  $m/2$ . The expected number of loops in a chain of  $n$  segments whose ends are at relative extension  $y$ ,  $W_0(n, y)$ , is therefore  $P(m, m/2; p)$  summed over all values of  $m$ :

$$W_0(n, y) = \sum_{m=2}^n \frac{m!}{[(m/2)!]^2} [p(1-p)]^{m/2} \quad (\text{A6})$$

The probability that there is at least one loop in the chain, assuming a Poisson distribution of the number of loops, is then

$$W_1(n, y) = 1 - \exp[-W_0(n, y)] \quad (\text{A7})$$

We expect to begin to see short-range interactions between DNA segments separated along the chain when  $W_1(n, y)$  is significantly greater than zero.

The inverse of the Langevin function

$$L^*(x) = \coth(x) - \frac{1}{x} \quad (\text{A8})$$

has the following series expansion, which is accurate to 0.25%:

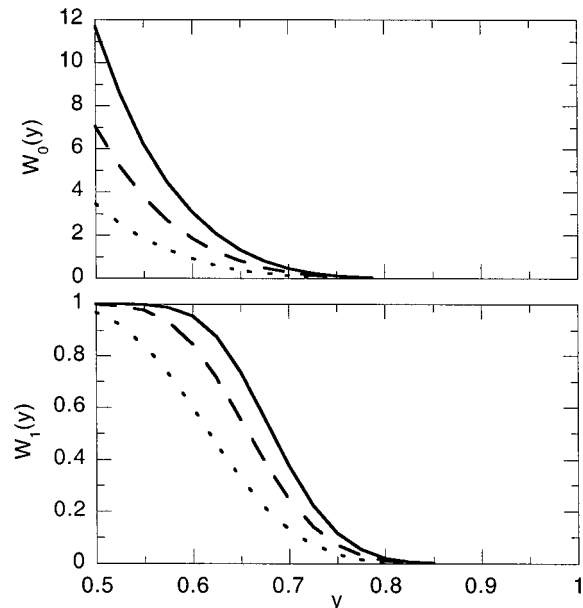


FIGURE 11 Average number of loops  $W_0$  (upper graph) and probability  $W_1$  of at least one loop (lower graph) as function of fractional maximum extension  $y = x/x_{\max} = x/nl$  in chains containing (top to bottom)  $n = 164$ , 100, and 50 statistical segments. The probability  $W_1$  becomes appreciably greater than zero for fractional maximum extensions in the range 0.7 to 0.8. For  $\lambda$  DNA, with maximum extension  $16.4 \mu\text{m}$  in B form geometry, this corresponds to an extension of  $11.5$  to  $13.1 \mu\text{m}$ . This is in good agreement with the observed extensions at which a constant but non-zero force is first observed, buttressing the interpretation that this is the region in which short-range interactions between segments of the same DNA molecule can first occur.

$$L^*(y) = 3y + \frac{9}{5}y^3 + \frac{297}{175}y^5 + \frac{1539}{875}y^7 + \frac{126117}{67375}y^9 + \frac{43733439}{21896875}y^{10} \quad 0 \leq y \leq 0.537 \quad (\text{A9a})$$

$$= -1.037 + 5.660y + 9.376(y - c)^2 + 17.04(y - c)^3 + 52.02(y - c)^4 + 94.86(y - c)^5 \quad 0.537 < y \leq 1 \quad (\text{A9b})$$

where  $c = 0.5366$ . We use this expansion in Eqs. A2-A4 to obtain  $p(y)$ , and substitute this value in Eqs. A6 and A7 to obtain the desired probability of at least one loop. The results for chains containing  $n = 50, 100$ , and 164 statistical segments are shown in Fig. 11.

C. G. Baumann thanks I. Rouzina for many helpful discussions and S. Fiddler for her hospitality during visits to the University of Oregon. M. W. and S. B. thank Dr. Eric Siggia for his helpful advice. This work was supported in part by National Science Foundation grant MBC 9118482 and National Institutes of Health grant GM 32543 to C. Bustamante, National Institutes of Health Grant GM 28093 to V. Bloomfield, and an National Institutes of Health Traineeship (GM 08277) to C. G. Baumann; and by the Cancer Research Fund of the Damon Runyon - Walter Winchell Foundation fellowship, DRG-1326 to M. D. Wang.

## REFERENCES

- Arcsott, P. G., C. Ma, J. R. Wenner, and V. A. Bloomfield. 1995. DNA condensation by cobalt hexaammine(III) in alcohol-water mixtures: dielectric constant and other solvent effects. *Biopolymers*. 36:345-364.
- Baumann, C. G., S. B. Smith, V. A. Bloomfield, and C. Bustamante. 1997. Ionic effects on the elasticity of single DNA molecules. *Proc. Natl. Acad. Sci. USA*. 94:6185-6190.
- Benbasat, J. A. 1984. Condensation of bacteriophage  $\phi$ W14 DNA of varying charge densities by trivalent counterions. *Biochemistry*. 23:3609-3619.
- Bloomfield, V. A. 1991. Condensation of DNA by multivalent cations: considerations on mechanism. *Biopolymers*. 31:1471-1481.
- Bloomfield, V. A. 1996. DNA condensation. *Curr. Opin. Struct. Biol.* 6:334-341.
- Bloomfield, V. A. 1997. DNA condensation by multivalent cations. *Biopolymers*. 44:269-282.
- Braunlin, W. H., T. J. Strick, and M. T. Record, Jr. 1982. Equilibrium dialysis studies of polyamine binding to DNA. *Biopolymers*. 21:1301-1314.
- Bustamante, C., J. F. Marko, E. D. Siggia, and S. Smith. 1994. Entropic elasticity of lambda-phage DNA. *Science*. 265:1599-1600.
- Cook, P. R. 1994. RNA polymerase: structural determinant of the chromatin loop and the chromosome. *BioEssays*. 16:425-430.
- Flory, P. J. 1953. Principles of Polymer Chemistry. Cornell University Press, Ithaca, NY.
- Gosule, L. C., and J. A. Schellman. 1976. Compact form of DNA induced by spermidine. *Nature*. 259:333-335.
- Gronbech-Jensen, N., R. J. Mashl, R. F. Bruinsma, and W. M. Gelbart. 1997. Counterion-induced attraction between rigid polyelectrolytes. *Phys. Rev. Lett.* 78:2477-2480.
- Grosberg, A. Y., and A. R. Khokhlov. 1994. Polyelectrolytes. Trans. Atanov, Y. A. In *Statistical Physics of Macromolecules*. American Institute of Physics Press, New York. 3,5,217-220.
- Hagerman, P. J. 1988. Flexibility of DNA. *Annu. Rev. Biophys. Biophys. Chem.* 17:265-286.
- Halperin, A., and E. B. Zhulina. 1991. Stretching polymer brushes in poor solvents. *Macromolecules*. 24:5393-5397.
- James, H. M., and E. Guth. 1943. Theory of the elastic properties of rubber. *J. Chem. Phys.* 11:455-481.
- Kovac, J., and C. C. Crabb. 1982. Modified gaussian model for rubber elasticity. 2. The worm-like chain. *Macromolecules*. 15:537-541.
- Ma, C., L. Sun, and V. A. Bloomfield. 1995. Condensation of plasmids enhanced by Z-DNA conformation of d(CG)n inserts. *Biochemistry*. 34:3521-3528.
- Manning, G. S. 1978. The molecular theory of polyelectrolyte solutions with applications to the electrostatic properties of polynucleotides. *Q. Rev. Biophys.* 11:179-246.
- Manning, G. S. 1980. Thermodynamic stability theory for DNA doughnut shapes induced by charge neutralization. *Biopolymers*. 19:37-59.
- Manning, G. S. 1985. Packaged DNA: an elastic model. *Cell. Biophys.* 7:57-89.
- Marko, J. F., and E. D. Siggia. 1995. Stretching DNA. *Macromolecules*. 28:8759-8770.
- Marquet, R., and C. Houssier. 1991. Thermodynamics of cation-induced DNA condensation. *J. Biomol. Struct. Dynam.* 9:159-167.
- Oberhauser, A. F., P. E. Marszalek, H. P. Erickson, and J. M. Fernandez. 1998. The molecular elasticity of the extracellular matrix protein tenascin. *Nature*. 393:181-185.
- Odijk, T. 1995. Stiff chains and filaments under tension. *Macromolecules*. 28:7016-7018.
- Oosawa, F. 1968. Interaction between parallel rodlike macroions. *Biopolymers*. 6:1633-1647.
- Ostrovsky, B., and Y. Bar-Yam. 1995. Motion of polymer ends in homopolymer and heteropolymer collapse. *Biophys. J.* 68:1694-1698.
- Plum, G. E., P. G. Arcsott, and V. A. Bloomfield. 1990. Condensation of DNA by trivalent cations. 2. Effect of cation structure. *Biopolymers*. 30:631-643.
- Plum, G. E., and V. A. Bloomfield. 1988. Equilibrium dialysis study of binding of hexaammine cobalt(III) to DNA. *Biopolymers*. 27:1045-1051.
- Post, C. B., and B. H. Zimm. 1979. Internal condensation of a single DNA molecule. *Biopolymers*. 18:1487-1501.
- Post, C. B., and B. H. Zimm. 1982a. Light scattering study of DNA condensation: Competition between collapse and aggregation. *Biopolymers*. 21:2139-2160.
- Post, C. B., and B. H. Zimm. 1982b. Theory of DNA condensation: collapse vs. aggregation. *Biopolymers*. 21:2123-2137.
- Quake, S. R., H. Babcock, and S. Chu. 1997. The dynamics of partially extended single molecules of DNA. *Nature*. 388:151-154.
- Rau, D. C., and V. A. Parsegian. 1992. Direct measurement of the intermolecular forces between counterion-condensed DNA double helices: evidence for long range attractive hydration forces. *Biophys. J.* 61:246-259.
- Reich, Z., R. Ghirlando, and A. Minsky. 1991. Secondary conformational polymorphism of nucleic acids as a possible functional link between cellular parameters and DNA packaging processes. *Biochemistry*. 30:7828-7836.
- Rief, M., M. Gautel, F. Oesterhelt, J. M. Fernandez, and H. E. Gaub. 1997. Reversible unfolding of individual titin immunoglobulin domains by AFM. *Science*. 276:1109-1112.
- Rief, M., J. Pascual, M. Saraste, and H. E. Gaub. 1999. Single molecule force spectroscopy of spectrin repeats: low unfolding forces in helix bundles. *J. Mol. Biol.* 286:553-561.
- Rouzina, I., and V. A. Bloomfield. 1996. Macroion attraction due to electrostatic correlation between screening counterions. 1. Mobile surface-adsorbed ions and diffuse ion cloud. *J. Phys. Chem.* 100:9977-9989.
- Rouzina, I., and V. A. Bloomfield. 1998. DNA bending by small, mobile multivalent cations. *Biophys. J.* 74:3152-3164.
- Saenger, W. 1984. Principles of Nucleic Acid Structure. Springer-Verlag, New York.

- Schnell, J. R., J. Berman, and V. A. Bloomfield. 1998. Insertion of telomere repeat sequence decreases plasmid DNA condensation by cobalt (III) hexaammine. *Biophys. J.* 74:1484–1491.
- Smith, S. B., Y. Cui, and C. Bustamante. 1996. Overstretching B-DNA: the elastic response of individual double-stranded and single-stranded DNA molecules. *Science*. 271:795–799.
- Stigter, D. 1998. An electrostatic model for the dielectric effects, the adsorption of multivalent ions, and the bending of B-DNA. *Biopolymers*. 46:503–516.
- Thomas, T. J., and V. A. Bloomfield. 1983. Collapse of DNA caused by trivalent cations: pH and ionic specificity effects. *Biopolymers*. 22: 1097–1106.
- Wang, M. D., H. Yin, R. Landick, J. Gelles, and S. M. Block. 1997. Stretching DNA with optical tweezers. *Biophys. J.* 72:1335–1346.
- Widom, J., and R. L. Baldwin. 1980. Cation-induced toroidal condensation of DNA: studies with  $\text{Co}^{3+}(\text{NH}_3)_6$ . *J. Mol. Biol.* 144:431–453.
- Wilson, R. W., and V. A. Bloomfield. 1979. Counterion-induced condensation of deoxyribonucleic acid. A light-scattering study. *Biochemistry*. 18:2192–2196.
- Yin, H., M. D. Wang, K. Svoboda, R. Landick, S. M. Block, and J. Gelles. 1995. Transcription against an applied force. *Science*. 270:1653–1657.
- Yoshikawa, K., S. Kidoaki, M. Takahashi, V. V. Vasilevskaya, and A. R. Khokhlov. 1996a. Marked discreteness on the coil-globule transition of single duplex DNA. *Berichte der Bunsen Gesellschaft für Physikalische Chemie*. 100: 876–880.
- Yoshikawa, K., M. Takahashi, V. V. Vasilevskaya, and A. R. Khokhlov. 1996b. Large discrete transition in a single DNA molecule appears continuous in the ensemble. *Phys. Rev. Lett.* 76:3029–3031.